

One-dimensional photonic crystals (Si/SiO₂) for ultrathin film crystalline silicon solar cells

S. Saravanan, R. S. Dubey

Advanced Research Laboratory for Nanomaterials & Devices, Department of Nanotechnology, Swarnandhra College of Engineering & Technology, Seetharamapuram, Narsapur – 534 280, West Godavari, Andhra Pradesh, India

shasa86@gmail.com

PACS 73.50.h, 84.60.Jt

DOI 10.17586/2220-8054-2020-11-2-189-194

The performances of ultrathin film silicon solar cells are limited due to low light absorption and poor collection of charge carriers. In this work, we have designed and studied the one-dimensional photonic crystals (1DPCs) and thin film silicon solar cells. For the simulation, the plane wave method (PWM) and rigorous coupled wave analysis (RCWA) methods were used. First, we explored the analysis of bandgap, field distribution and the reflectivity of 1DPCs. Later, the optimized Si/SiO₂ 1DPC was integrated with the crystalline silicon solar cell as the back reflector and simulation was performed. The performance of designed solar cells showed the strong influence of 1DPC. The solar cell is integrated with the three distributed Bragg reflectors (5DBRs) at the bottom showed the best performance with its enhanced short circuit current and cell efficiency.

Keywords: PWM, 1DPC, bandgap, RCWA, cell efficiency.

Received: 30 November 2019

Revised: 26 December 2019

1. Introduction

Renewable energy resources are needed to save the environment and for clean energy production (electricity). Researchers and environmentalists have been focusing on photonic crystals (PCs) which are nothing than artificial periodic dielectric structures. Such PCs possess the different refractive indices of their materials. A properly designed and fabricated photonic crystal prohibits the propagation of the electromagnetic waves. The photonic crystals are classified as one- (1D), two- (2D) and three-dimensional (3D) according to their periodicity. Over last few decades, the dielectric layers have been in wide demand for use in several applications, such as thin film solar cells, LEDs, thermal collector, optical filter, reflective coatings, optical buffer, and optical computers [1–8]. The performance of the photonic crystals has been studied by using various simulation techniques such as plane wave method (PWM), rigorous coupled-wave analysis (RCWA), transfer matrix method (TMM), finite-difference time-domain (FDTD) and Finite element method (FEM) [9–11]. Use of 1DPC as the back reflector in thin film solar cells showed the improved light absorption. Dubey and Ganesan (2017) experimentally prepared and studied the SiO₂/TiO₂ based multilayer structures by using sol-gel spin coating method. The refractive indices of SiO₂ and TiO₂ layers were 1.43 and 2.0 with layer thicknesses of 230 and 70 nm each. They achieved ~ 78 % reflectance with the composition of six low and high dielectric layers of SiO₂ and TiO₂ respectively at center wavelength (λ) 829 nm [12]. Chen et al. (2014) designed and demonstrated the one-dimensional photonic crystals as the back reflectors for thin-film silicon solar cells. The plane wave expansion (PWE) and the FDTD method were used to study the photonic bandgap properties. Further, the optical properties of reflection and absorption of 1DPCs were studied. They reported the reflectivity ~ 97 % by using five distributed Bragg reflectors (5DBRs). The designed solar cell with 5DBRs showed the influence of refractive index contrast and the thickness of the layers and produced 13.41 % mA/cm² [13]. Sheng et al. (2010) presented the silicon solar cells with the integration of porous aluminum and distributed Bragg's reflector (DBR) as the back reflectors. This design showed an improvement in photovoltaic performance more than 50 % as compared to reference cell [14]. Again Sheng et al. (2012) demonstrated the design of thin-film solar cell structures by using various back reflectors. The DBR was consisting of amorphous-Si and SiO₂ films with their corresponding refractive indices 3.6 and 1.45 designed at center wavelength at 800 nm. However, the improved solar cell performance was attributed to the diffraction grating and DBR integrated at the bottom of solar cell [15]. In this paper, we present the design of Si/SiO₂ 1DPCs and ultrathin film crystalline silicon solar cells. The use of DBR showed the enhancement in light absorption and hence, the cell efficiency. The designing of 1DPCs and ultrathin crystalline silicon solar cells are presented in Section 2 while the simulated results are discussed in Section 3. Finally, paper is summarized in Section 4.

2. Designing approach

Figure 1 shows the proposed design of ultrathin crystalline silicon solar cells. This solar cell design was consist of Si_3N_4 antireflection coating (ARC), Al substrate, SiO_2 buffer layer, Al/ITO dual gratings (bottom & top) and 1DPCs (Si/SiO_2). The thicknesses of each component was as below: ARC 70 nm (t_8), top grating 50 nm (t_7), Silicon absorber 41 nm (t_6), bottom grating 159 nm (t_5) and buffer layer 57 nm (t_4) whereas the thicknesses of Si and SiO_2 were 57 nm (t_3) and 137 nm (t_2) respectively. The substrate thickness of Al was 200 nm (t_1).

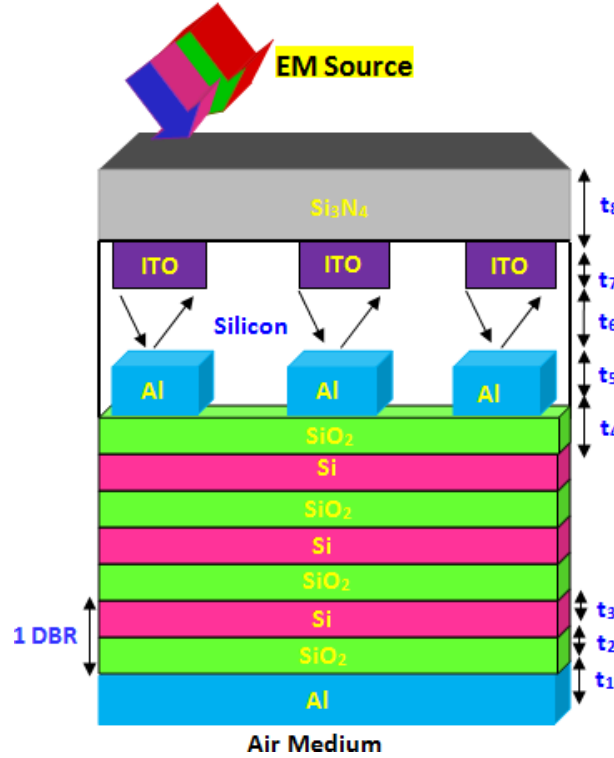


FIG. 1. The schematic diagram of DBR integrated with ultrathin amorphous silicon solar cell

The absorbing material was crystalline silicon with a thickness of approximately 41 nm. Here, the SiO_2 buffer layer was integrated between the DBR and the crystalline silicon absorbing layer. The FDTD technique is widely used for electromagnetic wave analysis. This technique divides the time and space at regular spatial grid size intervals and the simulation time evolve in the field. For the simulation, periodic boundary conditions for X- and Y-axis and the perfect matched layer for Z-axis were applied. Using the optimized design of 1DPC by using plane wave method (PWM), we have presented the solar cells design with the integration of DBR at the bottom and the various analyses were explored using RCWA method.

3. Results and discussion

Figure 2 shows the photonic bandgap (PBG) diagram of 1DPCs by varying the number of stacks (S) of Si/SiO_2 and the thicknesses 57 nm (t_3) and 137 nm (t_2) respectively designed at center wavelength 800 nm. The choice of a large dielectric contrast material is desirable have a wider bandgap. Here, our chosen materials are Si ($n_1 = 3.4$) and SiO_2 ($n_2 = 1.45$), because of their large refractive index contrast. For the simulation of 1DPC, we applied the periodic boundary conditions (PBC) in the Z-axis and the perfect matched layers (PML) in the X- and Y-axis. In the PBG diagram, as shown in Fig. 1, the X-axis represents the K-wave vector, whereas, the Y-axis represents the eigen frequencies ($\omega a/2\pi c$). Here, ω is the frequency, c is the speed of light in a vacuum, and a is the lattice constant. We can clearly observe the effect of increased number of stacks. As the thickness was increased the bandwidth of the photonic band was decreased. Table 1 shows the analysis of PBG by varying the number of stacks and their reflection bandwidth.

As much as 99 % reflectivity was achieved from the photonic crystals (PCs) based on 5 stacks of Si/SiO_2 layers. The PBGs are strongly dependent on the different variables, for example, the refractive index (n), period (N), dielectric constant (ϵ) etc. To realize the field distribution in the number of stacks, we have plotted the diagram Fig. 3. We can

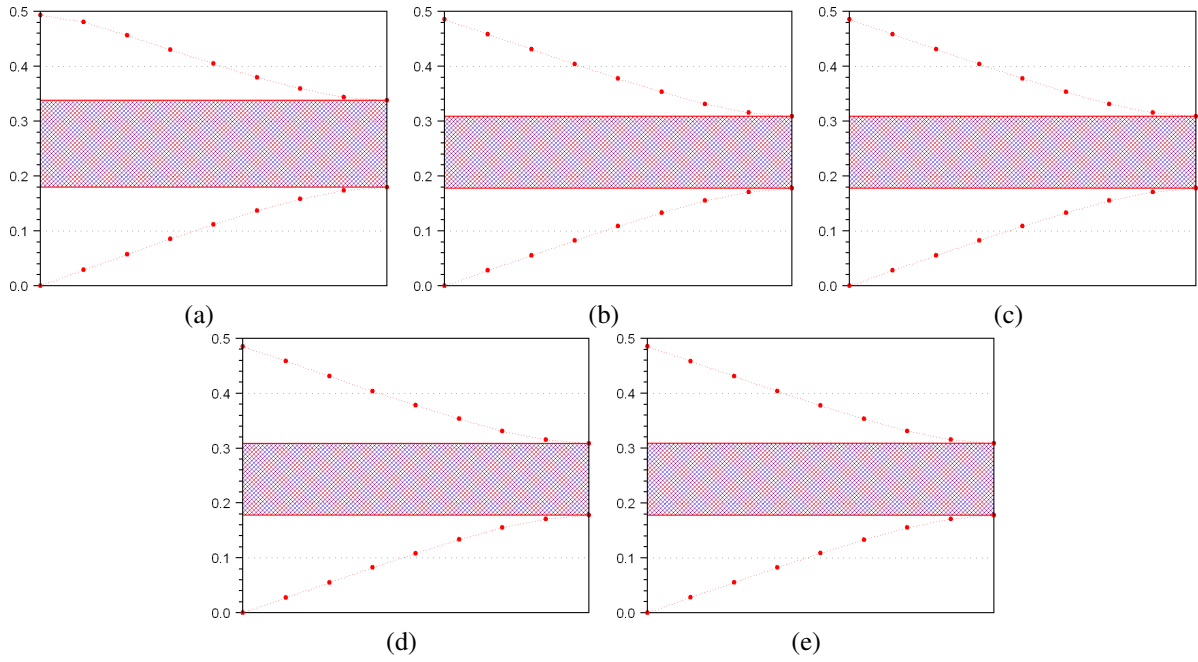


FIG. 2. Photonic bandgap of 1DBR (a), 2DBR (b), 3DBR(c), 4DBR (d) and 5DBR (e)

TABLE 1. The photonic bandgap, reflection and field intensity of Si/SiO 1DPC structures

DBR	Photonic Band Gap / Frequency ($\omega a/2\pi c = a/\lambda$)	Reflection (%)	Field Intensity
1S	0.16	49.3	1.70
2S	0.13	87.8	1.92
3S	0.13	96.8	1.98
4S	0.13	98.5	1.98
5S	0.13	98.8	1.98

assume that the light was irradiated from the left side and the field distribution was studied within the 1S, 2S, 3S, 4S and 5S of Si/SiO₂ stacks. The RCWA method is useful for the field distribution analysis and the reflectivity of the various stacks as shown in Fig. 3. The incident light on the dielectric medium shows the partial reflection and partial transmission the light. Consequently, the transmission of light was decreased due to the total internal reflection of incident light with the increased number of stacks. This phenomenon plays a key role when 1DPC is integrated as a back reflector in thin film solar cell. It gives the folding of unabsorbed light passed through the active region and therefore, increases the light absorption in longer wavelength.

Referring to Fig. 3(a–e), we can observe the field distribution or gradual decrease in the light intensity from the left to right side. The red and pink color strips can be understood as the high and low intensity of field from left to right side as shown in Fig. 3(a–e). We can observe the shifting and widening of reflection band with the increased of the number of stacks as shown in Fig. 3(f). As much as about 99 % reflection was observed from the photonic crystal based on 5 stacks. The reflectivity corresponding to 1S, 2S, 3S, 4S and 5S were 49.3, 87.8, 96.8, 98.5, 98.85 %. Table 1 summarizes the bandgap, reflectivity and field intensities. With this analysis of reflection using N-stacks, we have integrated this structure at the bottom of solar cell as represented in Fig. 1.

Figure 4 shows the bar diagram of cell efficiency of various solar cells by varying the number of 1DPC stacks as the back reflector. We can clearly observe the enhancement in the cell efficiency with respect to the increased Si/SiO₂ stacks as compare to designed solar cell without photonic crystals or back reflector for the transverse electric mode (TE). Generally, the thin-film solar cells do not have the capability to absorb light in the longer wavelength region and therefore it severely affects the conversion efficiencies of solar cells. The role of 1DPCs is to act as back reflector for the wavelength region which could not be absorbed in the absorbing medium. Similar trends are observed for the transverse magnetic (TM) waves. However, for the case of TM wave the cell efficiency was better than the transverse electric (TE) wave case. This enhancement is attributed to the bottom metal (Al) grating which generated the surface

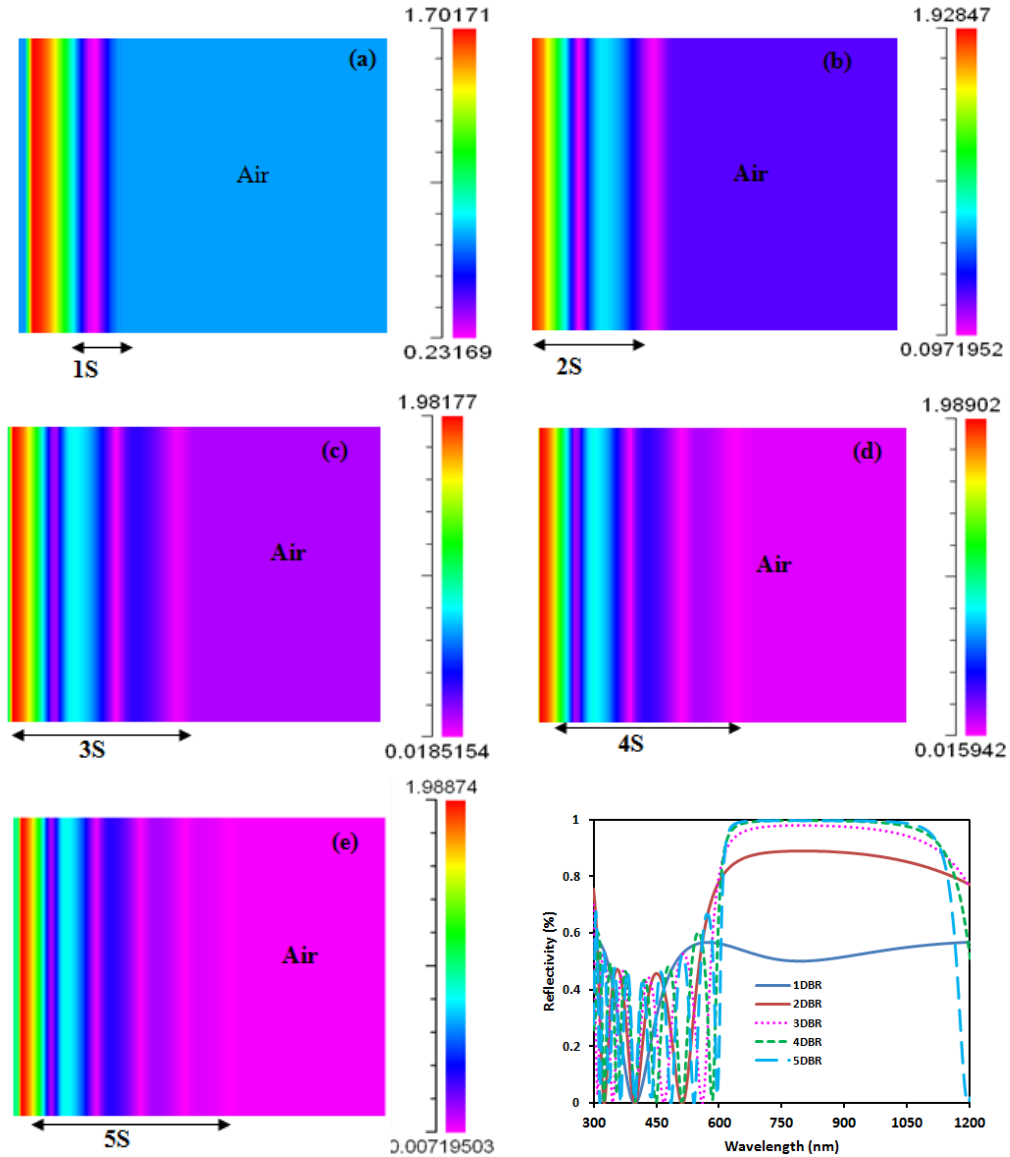


FIG. 3. Transverse electric (TE) field distribution of 1S (a), 2S (b), 3S (c), 4S (d), 5S (e) with intensity profile and reflectivity (f)

plasmons and localization of the field. The designed solar cell using 1DPC based on three stacks showed the maximum photovoltaic performance i.e. short-circuit current (J_{SC}) 19.69 and 25.54 mA/cm² while cell efficiency (η) 16.8 and 19.5 % for the case of TE and TM waves respectively. The light trapping plasmonic nanostructures are the important factor to enhance the optical performance [16].

The use of 1DPC is to enhance the light absorption by folding the light back to the Si absorber region. In this context, we have studied the light absorption for the case of TE and TM waves which is plotted in Fig. 5. From this figure, we can clearly observe the enhancement of light absorption in the solar cell based on 3S-1DPC. Comparably, the light absorption for the TM case is dominant which is due to the induced surface plasmons with the localized field at the tip of the Al grating as shown in the inset of Fig. 5 at the right-hand side. The use nanogratings were found to be important in order to enhance the light trapping in the multiple junctions [17–19]. Here, the Al and ITO gratings are supposed to have the scattering of light with the large diffraction angle for prolonging the photon pathlength. The analysis of TE and TM depicts the nature of light within the simulated structure. The electric field distribution at 460 nm shows the Fabry–Perot resonance and guided modes in the absorber region due to the back reflector, remarkably. Similarly, magnetic field distribution at wavelength 840 nm confirmed the localized surface

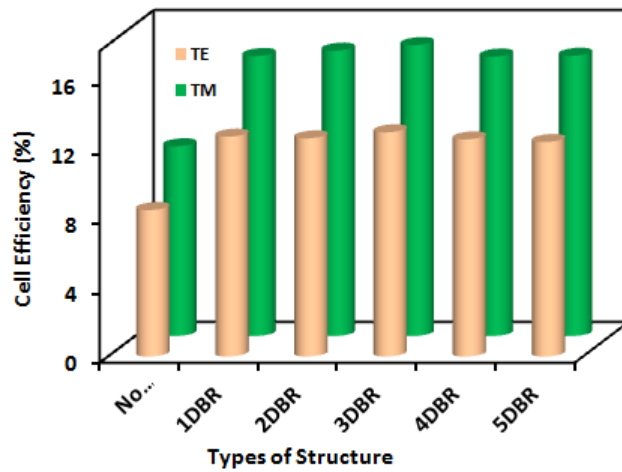


FIG. 4. Bar diagram of solar cell efficiency (TE & TM cases) of various solar cells

plasmons and the surface guided modes observed in the absorber region. It represents significant enhancement of light trapping due to the combined photonic and plasmonic effects.

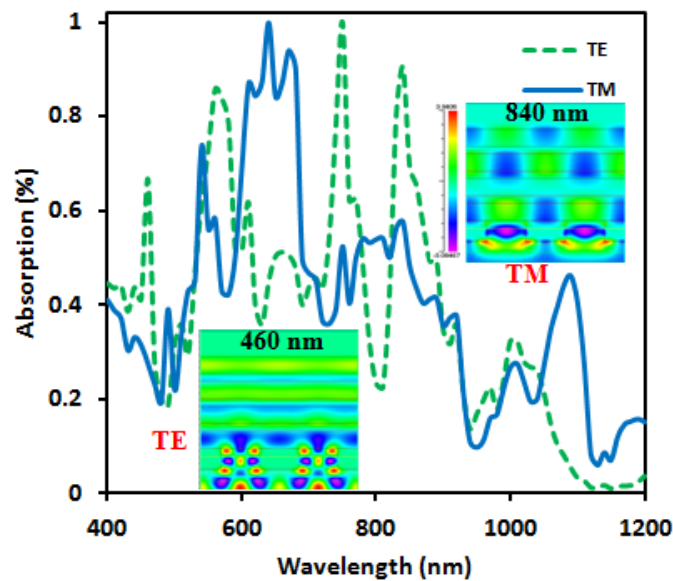


FIG. 5. The absorption spectrum of 3-stacks based ultrathin silicon solar cell in both polarization modes

4. Conclusion

In this work, designing of 1DPC with respect to the number of stacks and thin-film silicon solar cell has been presented. The photonic bandgap was found to be shifted towards the longer wavelength with its widening as a function of increased number of stacks. The proposed design of solar cell based on 3S-1DPC showed the enhanced short-circuit current density and solar cell efficiency. This enhancement was attributed to the light trapping mechanism supported by the 1DPC as the back reflector and the guiding of light by the diffraction grating of ITO on the top and Al at the bottom. For the TM case, the field distribution was significantly enhanced due to the induced surface plasmons which could contribute to the enhanced photovoltaic performance. Finally, the proposed design of thin film solar cell is useful for the enhancement of light absorption assisted by the photonic and plasmonic modes.

References

- [1] Banerjee A. Novel applications of one-dimensional photonic crystal in optical buffering and optical time division multiplexing. *Optik*, 2001, **122** (4), P. 355–357.
- [2] Saravanan S., Dubey R.S., Kalainathan S. Design and optimization of ultrathin crystalline silicon solar cells using an efficient back reflector. *AIP advances*, 2015, **5**, 057160-10.
- [3] Yong K., Yu H.K., et al. Flexible top-emitting diodes with a functional dielectric reflector on a metal foil substrate. *RSC advances*, 2018, **8**, P. 26156–26160.
- [4] Mu C., Cornelissen H.J., Bociort F., Liebig T. Dielectric multilayer angular filters for coupling LEDs to thin light guides. *Proceedings of SPIE*, 2011, **8170**, 817001-1-6.
- [5] Kumar M., Kumari N., et al. Multilayer dielectric thin-film optical filters for beam folding applications. *Proceedings of SPIE*, 2015, **9654**, 96540-1-5.
- [6] Yamamoto Y., Kamiys T., Yanai H. Characteristic of optical guided in multilayer metal-clad planar optical guide with low-index dielectric buffer layer. *IEEE Journal of Quantum Electronics* 1975, **11** (9), P. 729-736.
- [7] Young L. Multilayer reflection coatings on a metal mirror. *Applied Optics*, 1963, **2**, P. 445–447.
- [8] Chizari A., Abdollahramezani S., Jamali M.V., Salehi J.A. Analog optical computing based on a dielectric met-reflect array. *Optics Letters*, 2016, **41**, P. 3451–3453.
- [9] Meade R.D., Rappe A.M., et al. Accurate theoretical analysis of photonic bandgap materials. *Physics review B*, 1993, **48**, P. 843–8437.
- [10] Dubey R.S., Gautam D.K. Development of simulation tools to study optical properties of one-dimensional photonic crystals. *Journal of electromagnetic waves and applications*, 2012, **22** (5–6), P. 849–860.
- [11] Axmann W., Kuchment P. An efficient finite element method for computing spectra of photonic and acoustic bandgap materials. *Journal of Computational Physics*, 1999, **150**, P. 467–481.
- [12] Dubey R.S., Ganesan V. Reflectance modulation using SiO₂/TiO₂ multilayer structures prepared by sol-gel spin coating process for optical applications. *Superlattice and Microstructures*, 2017, **111**, P. 1099–1103.
- [13] Chen P., Hou G., et al. Optimal desing of on-dimensional photonic crystals back reflectors for thin film silicon solar cells. *Journal of Applied Physics*, 2014, **116**, 064508.
- [14] Sheng X., Johnson S.G., et al. Integrated photonic structures for light trapping in thin film Si solar cells. *Applied Physics Letters*, 2012, **100**, 111110-1-3.
- [15] Sheng X., Liu J., et al. Integration of self-assembled porous alumina and distributed Bragg reflector for light trapping in Si photovoltaic devices. *IEEE photonics technology letters*, 2010, **22** (18), P. 1394–1396.
- [16] Zeng L., Yi Y., et al. Efficiency enhancement in Si solar cells by textured photonic crystal back reflector. *Applied Physics Letters*, 2006, **89**, 111111-1-3.
- [17] Sheng X., Liu J., et al. Integration of self-assembled porous alumina and distributed reflector for light trapping in Si photovoltaic devices. *IEEE photonics technology letters*, 2010, **22** (18), P. 1394–1396.
- [18] Krc J., Zeman M., Luxembourg S.L., Topic M. Modulated photonic crystal structures as broadband back reflectors in thin-film solar cells. *Applied Physics Letters*, 2001, **94**, 153501-1-3.
- [19] Dubey R.S., Sarojini P.L. Light trapping mechansim in one-dimensional (1D) photonic crystals for silicon-based solar cells. *Journal of Electromagnetic Waves and applications*, 2012, **27**, P. 1–9.